

# Testing and modeling HpGe detector with anti-Compton shield

N.T. Tursunbayev<sup>\*,1,3</sup>, B.A. Urazbekov<sup>1,2,3,4</sup>

<sup>1</sup>Joint institute for nuclear research, Dubna, Russia

<sup>2</sup>Dipartimento di Matematica e Fisica, Università degli Studi della Campania "Luigi Vanvitelli", Caserta, Italy

<sup>3</sup>Dubna state university, Dubna, Russia

<sup>4</sup>Istituto Nazionale di Fisica Nucleare, Complesso Univeristario di Monte S. Angelo, Napoli, Italy

e-mail: tursunbayev.n@gmail.com

DOI: 10.29317/ejpfm.2020040303

Received: 05.09.2020 - after revision

Simulating with GEANT4 of anti-Compton shield containing eight BGO scintillators that works on anti-coincidence with HpGe detector was presented. The coefficient value of Compton tail suppression on <sup>60</sup>Co spectrum was taken by simulating and from experiment. Comparing results of experimental data with simulating were presented. The influence of anti-coincidence inclusion on the detector efficiency was determined with simulation.

**Keywords:** HpGe detector, BGO scintillators, GEANT4, anti-Compton shield

## Introduction

Modern  $\gamma$ -spectrometry provides unique opportunities for various research in many fields of knowledge, such as cosmic radiation, the study of the properties of solids, nuclear structures and activation analysis [1-4]. The main task of spectrometric measurements is to determine the energy, intensity of discrete  $\gamma$ -lines from various  $\gamma$ -sources, their identification and localization. However, the presence of natural and artificial backgrounds, the processes of scattering and absorption of  $\gamma$  radiation in the environment, and imperfection of the detecting equipment significantly complicate the solution of this problem. Therefore, for the reliable detection of  $\gamma$  -lines from various radionuclides,  $\gamma$ -spectrometry,

devices with the following properties are needed: good energy resolution, high speed, high registration efficiency at the peak of complete absorption, resistance to external factors, low cost.

Currently, various types of  $\gamma$ -detectors are used: semiconductor, scintillation, plastic, liquid, gas, etc. They differ significantly in their spectrometric properties, in operational characteristics and in technology and manufacturing cost. Among the  $\gamma$ -spectrometers, the leading position is undoubtedly occupied by semiconductor detectors, and in our example we use an HpGe detector (High purity Germanium) with an energy resolution on the  $\gamma$  line of 1.33 MeV ( $^{60}\text{Co}$ ) 1.8 keV and with a relative efficiency of 45 %.

## Interaction of gamma quantum with matter

At a sufficiently high energy of the  $\gamma$ -quantum, along with the photoelectric effect and the Compton effect, the formation of electron-positron pairs can occur. The process of pair formation cannot take place in a void, but requires the proximity of a nucleus or an electron. In the presence of a nucleus or an electron, the formation of a  $\gamma$ -quantum pair is possible, since it is possible to distribute the energy and momentum of the  $\gamma$ -quantum between three particles without contradicting the conservation laws. In this case, if the process of pair formation proceeds in the Coulomb field of the nucleus, then the energy of the recoil nucleus being formed turns out to be very small, so that the threshold energy required for the formation of a  $\gamma$ -quantum pair practically coincides with the doubled electron rest mass:  $E_\gamma = 1.022$  MeV. If the formation of electron-positron pairs takes place in the Coulomb field of an electron, then the threshold energy of the  $\gamma$ -quantum increases to  $E_\gamma = 2.044$  MeV. The cross section for the formation of electron-positron pairs in the nuclear field is as follows (Figure 1):

$$\sigma_{ee} = \frac{Z^2}{137} r_e^2 \left( \frac{28}{9} \ln \frac{2E_\gamma}{m_e c^2} - \frac{218}{27} \right), \quad (1)$$

where  $m_e c^2 \ll E_\gamma \ll 137 m_e c^2 Z^{-1/3}$  (without screening) and

$$\sigma_{ee} = \frac{Z^2}{137} r_e^2 \left( \frac{28}{9} \ln 183 Z^{-1/3} - \frac{2}{27} \right) \quad (2)$$

where  $E_\gamma \gg 137 m_e c^2 Z^{-1/3}$  (full screening), and  $137 m_e c^2 Z^{-1/3} = 22$  MeV for Ge. The dependence of the formation of electron-positron pairs on the charge is  $\sigma_{ee} \sim Z^2$ .

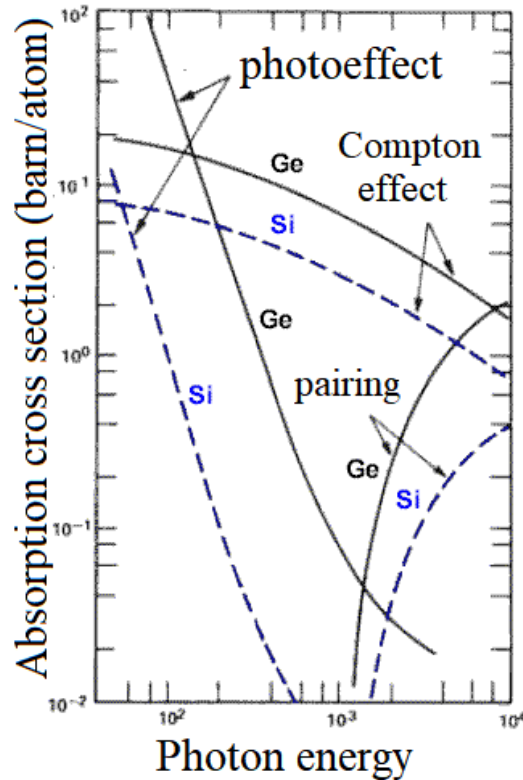


Figure 1. Energy dependence of the  $\gamma$  quantum interaction cross section with germanium and silicon [5].

## Peculiarities of detecting $\gamma$ -radiation

The photo-effect is the only process in which the energy of  $\gamma$  quanta is completely converted into the energy of electrons. However, the photo-effect is more likely to occur only at low energies, as seen in Figure 1. Compton scattering is dominant in a wide energy range. The scattered  $\gamma$ -quantum can leave the detector or interact with its mater if the detector is large enough. As a result of multiple interactions, the entire energy of the incident  $\gamma$ -quantum can be transferred to the detector.

The positron formed during the creation of a pair, leaving all the kinetic energy in the detector, annihilates into two  $\gamma$  quanta with an energy of 511 keV each. Annihilation  $\gamma$  -quanta fly relative to each other at an angle of  $180^\circ$ . This is a consequence of the law of conservation of momentum: the total momentum of  $\gamma$  -quanta must be equal to the momentum of the positron  $\vec{p}_{e^-} + \vec{p}_{e^+} = \vec{p}_{1\gamma} + \vec{p}_{2\gamma}$ , we assume that the electron is in a bound state, i.e.  $\vec{p}_{e^-} = 0$ , and the positron has a small momentum, since it transfers almost all the kinetic energy to the detector due to the Coulomb interaction  $\vec{p}_{e^+} \approx 0$ . It follows:

$$\vec{p}_{1\gamma} \approx -\vec{p}_{2\gamma} \quad (3)$$

In turn, these  $\gamma$ -quanta can be absorbed by the detector, or they can fly out of the detector. As a consequence, when registering monochromatic radiation, three peaks appear in the spectrum of the  $\gamma$ -quantum:  $E_\gamma$  is the peak of total absorption,  $E_\gamma - m_e c^2$  is the peak of single emission,  $E_\gamma - 2m_e c^2$  - double relegation peak.

In Figure 2 shows a simulation of the spectrum of registration of  $\gamma$ -quanta from the  $^{208}\text{Bi}$  radioactive source, with a characteristic  $\gamma$ -line of 2614.533 keV (Table 1). The peak with such an energy is the sum of events from photoabsorption and pair production with the absorption of both annihilation  $\gamma$  quanta. There are three more peaks on the Compton tail - 2103 keV, 1592 keV and 511 keV. The first of them caused due to the emission from the detector one annihilation  $\gamma$ -quantum, and the second one caused due to the emission from the detector both  $\gamma$ -quanta.  $^{208}\text{Bi}$  undergoes  $\beta^+$  decay or captures an electron from the inner shell:



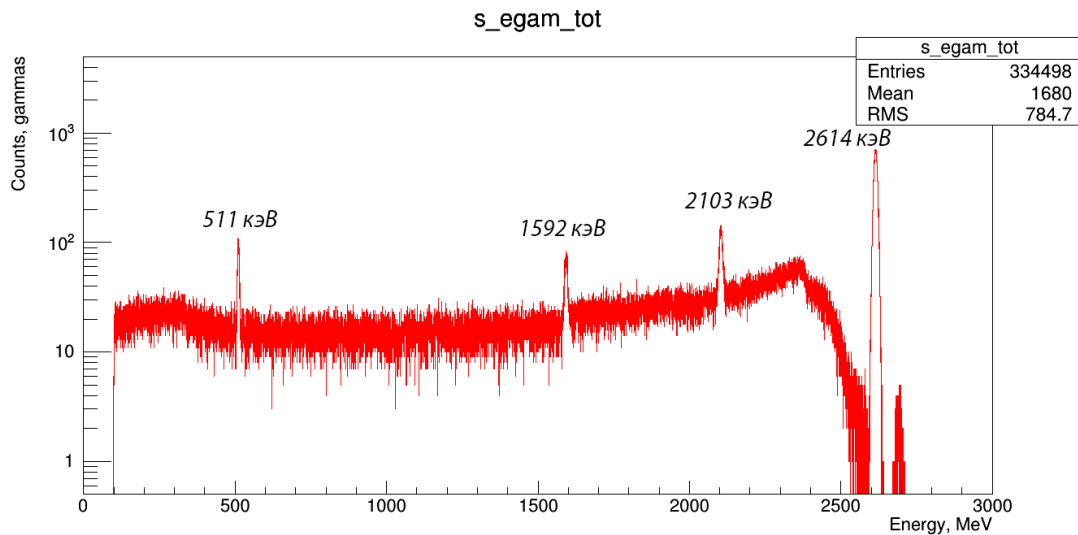
The positron from (5) annihilates with an electron and two  $\gamma$  quanta are formed, each with an energy of 511 keV, and one of them can enter the detector. The peak at 511 keV arises from these annihilation  $\gamma$  quanta.

Table 1.

Characteristic  $\gamma$ -lines  $^{208}\text{Bi}$  ( $T_{1/2} = 3.68 \cdot 10^5$  years).

$E_\gamma$ (keV)	Escape probability (%)	Decay type
2614.533	100	$\beta^+, EC$

In the simulation, the number of events is  $5 \cdot 10^7$ . The source was located at a distance of 15 cm from the germanium detector.

Figure 2. Simulation of the spectrum of the  $\gamma$ -quantum source  $^{208}\text{Bi}$ .

## Modeling with GEANT4

GEANT4 is a package of libraries for modeling radiation interactions that uses the Monte Carlo method. The Monte Carlo method is a numerical solution of mathematical problems by simulating random variables. The package began its development in the 70s of the last century at CERN. The need for such a package

was dictated by an increase in the complexity of experimental problems and the structure of installations. GEANT4 is free software. A lot of information about it, as well as its source code, can be found on the official [6, 7] website.

## Detector efficiency simulation

To calculate the efficiency of the detector exemplary spectrometric gamma sources are used. And, the presented in Table 2 elements were used for modeling.

Table 2.  
Exemplary spectrometric  $\gamma$ -sources.

Radionuclide ( $T_{1/2}$ , days)	Energy of $\gamma$ quanta, keV	Yield of $\gamma$ quanta decay
$^{44}\text{Ti}$ (21900)	1157,020	0,99875
$^{60}\text{Co}$ (1925,23)	1173,237	0,9985
	1332,501	0,999826
$^{88}\text{Y}$ (106,625)	898,036	0,939
	1836,052	0,9938
$^{133}\text{Ba}$ (3848,7)	276,3989	0,939
	302,8508	0,0716
	356,0129	0,6205
	383,8485	0,0894
$^{137}\text{Cs}$ (10990)	661,657	0,8499
$^{152}\text{Eu}$ (4941)	121,7817	0,2841
	344,2785	0,2658
	778,9045	0,1296
	964,072	0,1462
	1085,837	0,1013
	1112,076	0,1340
	1408,013	0,2085
$^{207}\text{Bi}$ (11800)	569,698	0,9776
	1063,656	0,7458
	1770,228	0,0687

The result of simulating detector efficiency as a function of energies is presented In Table 3. The source of  $\gamma$ -quanta is located at a distance of 15 cm from the germanium HpGe detector. The number of decays was given  $10^6$ . The efficiency was found by the formula

$$\varepsilon_{det} = \frac{N_{area}}{N_{total} \cdot \gamma} \quad (6)$$

where  $N_{area}$  is the area under the peak,  $N_{total}$  is the number of decays,  $\gamma$  is the probability of the  $\gamma$ -quantum emerging on one decay.

Table 3.

Detector efficiency with anticoincidence on and off.

Energy of $\gamma$ -quanta, keV, radionuclide	Detector efficiency (anticoincidence is on)	Detector efficiency (anticoincidence is off)
121.7817 $^{152}\text{Eu}$	0.0071	0.00713
276.3989 $^{133}\text{Ba}$	0.00446	0.00531
302.8508 $^{133}\text{Ba}$	0.00505	0.0048
344.2785 $^{152}\text{Eu}$	0.00405	0.00455
356.0129 $^{133}\text{Ba}$	0.00416	0.00406
383.8485 $^{133}\text{Ba}$	0.00422	0.00398
569.698 $^{207}\text{Bi}$	0.00285	0.00306
661.657 $^{137}\text{Cs}$	0.00269	0.00274
778.9045 $^{152}\text{Eu}$	0.00223	0.00255
898.036 $^{88}\text{Y}$	0.00214	0.00223
964.072 $^{152}\text{Eu}$	0.0021	0.00219
1063.656 $^{207}\text{Bi}$	0.00203	0.002
1085.837 $^{152}\text{Eu}$	0.00225	0.00236
1112.076 $^{152}\text{Eu}$	0.00205	0.00228
1157.020 $^{44}\text{Ti}$	0.00178	0.00188
1173.237 $^{60}\text{Co}$	0.00184	0.00194
1332.501 $^{60}\text{Co}$	0.00155	0.00174
1408.013 $^{152}\text{Eu}$	0.00164	0.00163
1770.228 $^{207}\text{Bi}$	0.00132	0.00134
1836.052 $^{88}\text{Y}$	0.00131	0.00133

Simulation of detector efficiency matches experimental data well and the dependence of efficiency on anti-Compton protection is weak: there is little difference between the graphs (Figure 3).

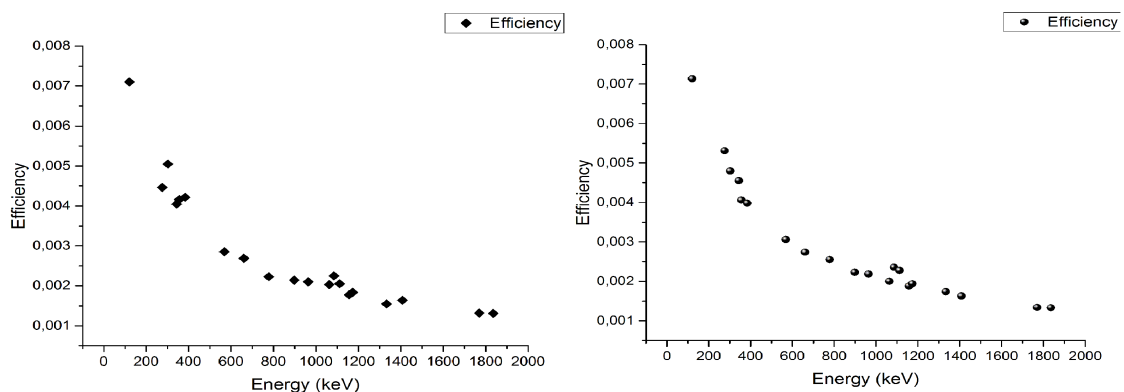


Figure 3. Simulation of detector efficiency with anticoincidences on (left) and off (right).

### Anti-Compton Defense Shield Modeling

The anti-Compton shield consists of eight BGO crystals, with an aluminum shell and a lead collimator (Figure 4). The collimator is 4 cm thick and is designed

to protect the scintillators from direct hit of  $\gamma$ -quanta from the source. The spectrum of  $\gamma$ -quanta on the BGO scintillator from  $^{60}\text{Co}$  with and without a lead collimator is showed on Figure 5. The BGO scintillator has a low energy resolution (14 % at 661 keV), so the two  $\gamma$  lines merged. In the energy range from 1050 keV to 1450 keV, the collimator reduces the number of  $\gamma$ -quanta by about 10 times. Hence it follows that without a collimator, the BGO scintillator can be triggered by other  $\gamma$ -quanta, when there is complete absorption in the germanium detector, this reduces true events.

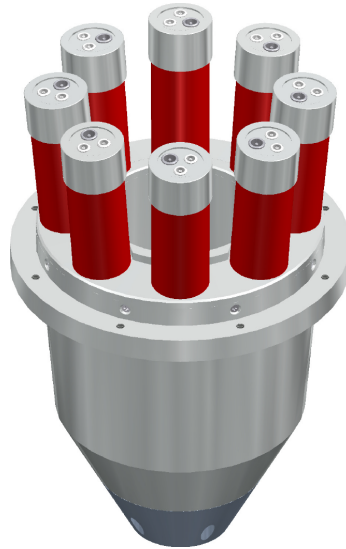


Figure 4. Detector system of eight BGO crystals, with an aluminum sheath and a lead collimator. Red tubes - photomultipliers.

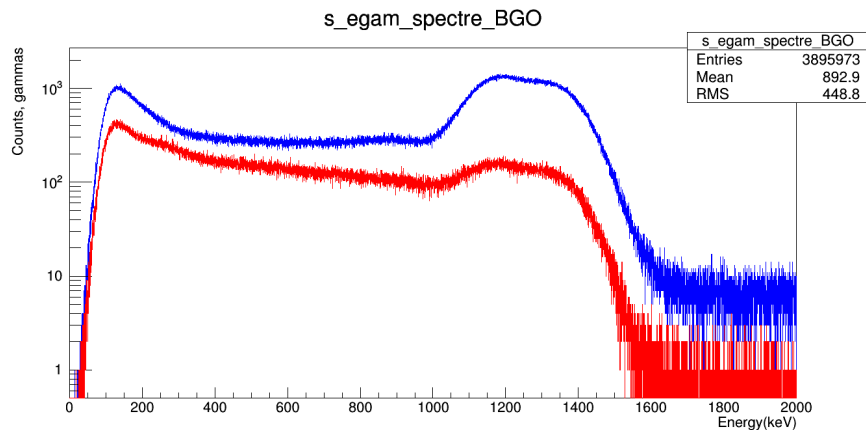


Figure 5. Simulation of the spectrum of  $\gamma$  quanta in the BGO scintillator from  $^{60}\text{Co}$  with a lead collimator (red lines) and without it (blue lines).

To obtain a good spectrum, the program has set the  $5 \cdot 10^7$  number of events, which means  $5 \cdot 10^7$  decays. In the case of  $^{60}\text{Co}$ , in almost every decay, 2  $\gamma$ -quant and 1 electron are emitted,  $10^8$   $\gamma$ -quant and  $5 \cdot 10^7$  electrons are emitted from the source. If the  $^{60}\text{Co}$  activity is 5 kBq, then to obtain  $5 \cdot 10^7$  events we need 3 hours of measurements.

All three sources of  $\gamma$ -quanta ( $^{60}\text{Co}$ ,  $^{207}\text{Bi}$ ,  $^{88}\text{Y}$ ) are located at a distance of 15 cm from the end of the germanium detector (Figures 6-7). The spectrum of  $^{60}\text{Co}$  has two distinct peaks with energies of 1173.237 keV and 1332.501 keV, they

are also called characteristic  $\gamma$ -lines. The Compton maximum has an energy of 962 (from 1173.237 keV) keV and 1117 keV (from 1332.501 keV). Above 1332.501 keV, a small number of events are present, this is due to the hitting of two  $\gamma$ -quanta on the detector at once. In the energy range from 100 keV to 1125 keV, the Compton tail is suppressed by a factor of 3.94. In the Compton peaks themselves in the energy range from 951 keV to 962 keV, the suppression coefficient increases to 6.42, and from 1115 keV to 1119 keV, the suppression coefficient increases to 5.5.

The spectrum of  $^{207}\text{Bi}$  has three characteristic  $\gamma$ -lines, with energies of 569.698 keV, 1063.656 keV and 1770.228 keV. A sharp drop in events above 1063.656 keV is associated with a low probability of the release of  $\gamma$ -photons with an energy of 1770.228 keV (6.87 %). Therefore, the peaks of single and double departure are not observed. The spectrum shows two Compton maxima with energies of 392 keV (from 569 keV) and 857 keV (from 1063.656 keV).

In the energy range from 100 keV to 560 keV, the Compton tail is suppressed by 3.49 times, in the range from 580 keV to 950 keV, the Compton tail is suppressed by 5.41 times. In the Compton peaks themselves in the energy range from 387 keV to 393 keV, the suppression coefficient increases to 5.35 and 849 keV to 858 keV, the suppression coefficient increases to 6.42.

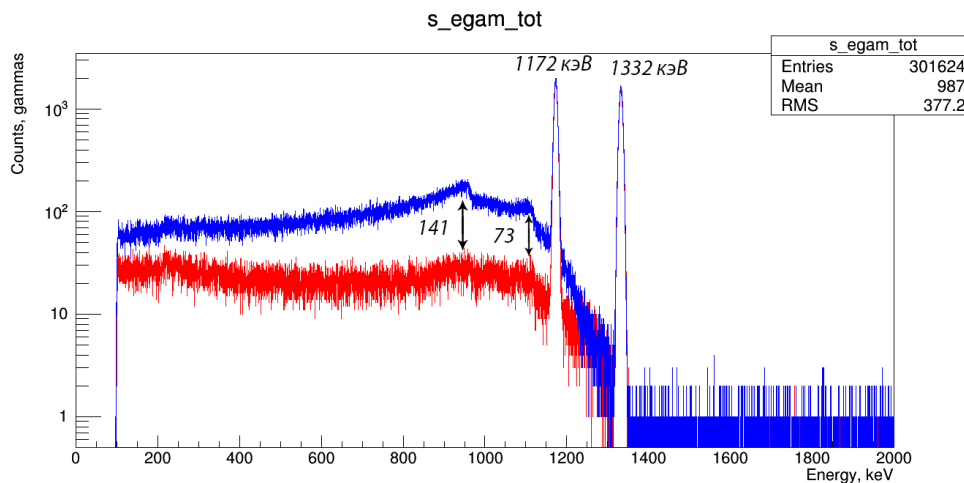


Figure 6. Simulation of the spectrum of  $^{60}\text{Co}$  with anticoincidence on (red lines) and off (blue lines).

The spectrum of  $^{88}\text{Y}$  has two characteristic  $\gamma$ -lines (898.036 keV and 1836.052 keV).

There are three more subtle peaks in the spectrum. The peak of the single emission from the  $\gamma$ -quantum with an energy of 1836 keV is located at 1325 keV, and the peak of the double emission corresponds to the energy of 814 keV. The peak with an energy of 511 keV, as indicated earlier in Figure 2, arises from annihilation  $\gamma$ -quanta. The Compton maximum has energies of 1611 (from 1836 keV) keV and 699 keV (from 898 keV).

In the energy range from 100 keV to 870 keV, the Compton tail is suppressed by a factor of 3.66, in the range from 920 keV to 1720 keV, the Compton tail is suppressed by a factor of 5.35. In the energy range from 511 keV to 512 keV, the suppression coefficient increases to 5.52, in the energy range from 687 keV to

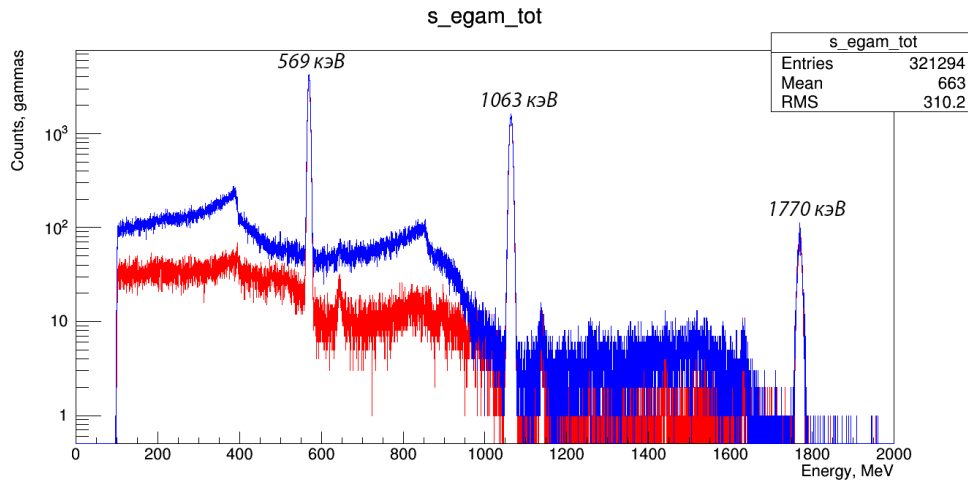


Figure 7. Simulation of the spectrum of  $^{207}\text{Bi}$  with anticoincidence on (red lines) and off (blue lines).

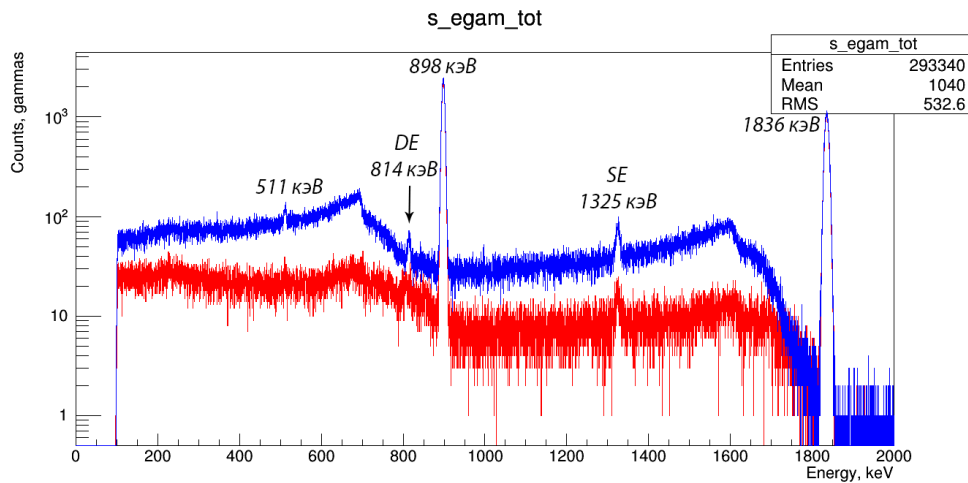


Figure 8. Simulation of the spectrum of  $^{88}\text{Y}$  with anticoincidence on (red lines) and off (blue lines).

699 keV, the suppression coefficient increases by 6.05 times, in the energy range from 1582 keV to 1611 keV, the suppression coefficient increases by 6.84 time. The simulation results are presented in Table 4.

Table 4.

Experimental values of the suppression coefficient for the  $^{60}\text{Co}$  spectrum.

Radionuclide	Energy interval, keV	Suppression coefficient
$^{60}\text{Co}$	150-1125	4.17
	951-962	6.42
	1115-1119	5.5
$^{88}\text{Y}$	100-870	3.66
	920-1720	5.35
	511-512	5.52
	687-699	6.05
	1582-1611	6.84
$^{207}\text{Bi}$	100-560	3.49
	580-950	5.41
	387-393	5.35
	849-858	6.42

## Experiment. Detector testing

The following settings were used in the experiment:

1. Coaxial HpGe Dewar detector filled with liquid nitrogen
2. BGO scintillator detector system
3. Digital signal recorder - "TsRS-32"
4. High voltage power supplies for HpGe and BGO
5. High-voltage switchgear for eight PMTs

The source of  $\gamma$  quanta (OSGI  $^{60}\text{Co}$ ) is located at a distance of 15 cm from the germanium detector. The HPGe detector is powered by a 3000V reverse voltage using a high voltage power supply. The high-voltage distributor is supplied with a positive voltage of 2000 V, from there the voltage is distributed to eight photomultipliers. The signals from the germanium detector go to the zero channel, and the signals from eight photomultipliers go to the first channel of "TsRS-32" (Figures 9, 10).

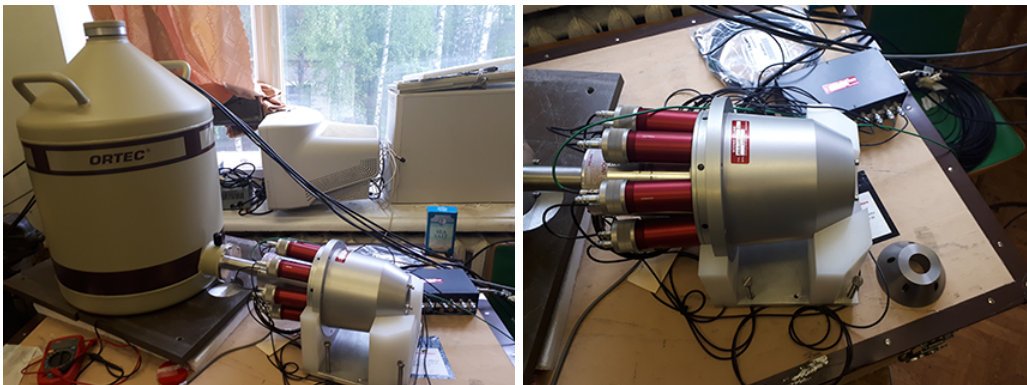


Figure 9. Assembling anti-Compton protection.



Figure 10. Digital signal recorder - "TsRS-32".

The digitizing frequency of TsRS-32 is 200 MHz. Hence, the time step in the histogram is 5 ns. Detailed technical parameters of OS-32 / TsRS-32 are given in the appendix.

The romana.x program manages all the data coming from the digital signal recorder and writes it to files. In the Channels tab, you can enable or disable channel numbers, set thresholds in each channel separately, lower and upper integration limits for peak and substrate, energy calibration factor for each channel. The Parameters tab sets the path for saving the file, the limit on the file size, sets the maximum and minimum values of the histogram for one event.

In the spectrum of  $^{60}\text{Co}$ , the Compton tail in the energy range from 150 keV to 1125 keV is suppressed by a factor of 2.76. In the energy range (951-962) keV, the suppression factor is 2.99 times, in the energy range (870-954) keV, the suppression factor is 4.2 times, in the energy range (1115-1119) keV, the suppression factor is 2.12 times.

Experiment results are presented in Table 5 and Figures 11, 12.

Table 5.

Experimental values of the suppression coefficient for the  $^{60}\text{Co}$  spectrum

Radionuclide	Energy interval, keV	Suppression coefficient
$^{60}\text{Co}$	150-1125	2.76
	951-962	2.99
	1115-1119	2.12
	870-954	4.2

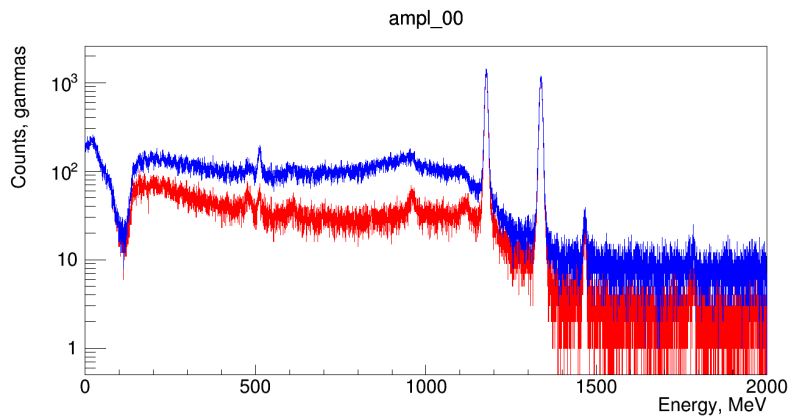


Figure 11. Spectrum of  $^{60}\text{Co}$  on HpGe with anticoincidence on and off.

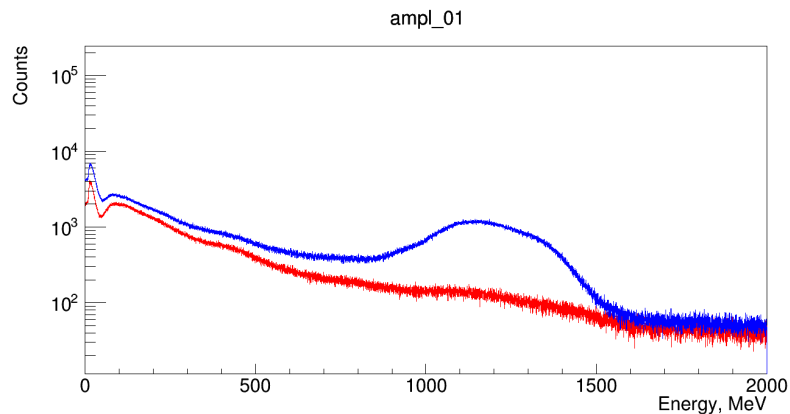


Figure 12.  $^{60}\text{Co}$  spectrum on BGO [8] with and without lead collimator.

## Comparison of simulation with experimental data

Comparisons of the collimator suppression coefficients from the simulation and from the experiment are given in Tables 6 and 7. The difference between the coefficients can be reduced by considering cosmic rays in the simulation.

Table 6.  
Pb collimator suppression coefficient values.

Radionuclide	Energy range, keV	Suppression factor	
		from experiment	from simulation
$^{60}\text{Co}$	150-900	1.69	2.04
	950-1400	7.95	8.56

Table 7.  
Suppression coefficient values for  $\gamma$  -sources.

Radionuclide	Energy range. keV	Suppression factor	
		from experiment	from simulation
$^{60}\text{Co}$	150-1125	2.76	4.17
	951-962	2.99	6.42
	1115-1119	2.12	5.5
	870-954	4.2	4.2
$^{88}\text{Y}$	100-870	–	3.66
	920-1720	–	5.35
	511-512	–	5.52
	687-699	–	6.05
	1582-1611	–	6.84
$^{207}\text{Bi}$	100-560	–	3.49
	580-950	–	5.41
	387-393	–	5.35
	849-858	–	6.42

## Conclusion

Modeling spectrometric systems is an important task for optimizing the geometry of an experiment, evaluating geometric corrections, and determining the efficiency of a detector system. In this work, a simulation of a  $\gamma$ -spectrometer consisting of an HpGe detector and anti-Compton protection was carried out using the GEANT4 software package. In the program, the real geometry of the detector systems was created, and point radioactive sources of  $\gamma$ -quanta were simulated. The obtained suppression coefficients of the Compton distribution from the simulation give satisfactory agreement with the experimental data, which allows the program to be used in the future for modeling and planning nuclear physics experiments.

## References

- [1] K.N. Muhin, Eksperimental'naya yadernaya fizika, T.1. Fizika atomnogo yadra. – 4-e izd. (Energoatomizdat, Moscow 1983) 616 p. (In Russian)
- [2] A.I. Abramov et al., Osnovy eksperimental'nyh metodov yadernoj fiziki. 3-e izd. (Energoatomizdat, Moscow 1985) 488 p. (In Russian)
- [3] Yu.K. Akimov, Poluprovodnikovye detektory yadernyh izluchenij ( Dubna: JINR, 2009) 207 p. (In Russian)
- [4] Yu.A. Cirlin et al., Optimizaciya detektirovaniya gamma-izlucheniya scintillyacionnymi kristalami (Energoatomizdat, Moscow 1991) 152 p. (In Russian)
- [5] Nuclear Physics in the Internet, <http://nuclphys.sinp.msu.ru>
- [6] Geant4 <http://geant4.cern.ch/>
- [7] ROOT Data Analysis Framework <https://root.cern.ch/>
- [8] <http://www.niic.nsc.ru/science/razrabotki/619-materials/bgo/1734-bgo/>